Motivating the Use of Dynamic Line Ratings to Mitigate the Risk of Wildfire Ignition

Shubham Tandon, Santiago Grijalva, and Daniel K. Molzahn
Georgia Institute of Technology
Atlanta, Georgia, 30318, USA

***Abstract*—Increasingly severe wildfires pose significant dangers to ecological, social, and economic systems. To curtail the risk of igniting wildfires, California utilities employ the Public Safety Power Shutoff (PSPS) program, which de-energizes transmission lines that run through wildfire-prone regions. In order to reduce the amount of load shedding required during PSPS events, this paper explores the use of dynamic line ratings (DLR) to manage the current flows on lines that pose a high risk of igniting wildfires. DLR schemes determine line flow limits that change with ambient conditions. This paper uses DLR in combination with more restrictive ground clearance requirements during wildfire-prone conditions to reduce the likelihood of wildfire-igniting faults from conductors contacting vegetation. Using two case studies, this paper demonstrates the potential benefits of DLR in this context by comparing the tradeoffs between completely de-energizing lines versus imposing more stringent ground clearance requirements via reducing current flows with DLR. Results from a large dataset representing WECC with actual data regarding ambient conditions, load demands, and wildfire risks show that the proposed approach can significantly reduce load shedding due to de-energizing lines that pose high risks of igniting wildfires.**

***Index Terms*—Overhead lines, dynamic-line rating, ampacity, wildfire mitigation, unit commitment**

I. Introduction

Wildfires have become increasingly intense phenomena due to drought conditions in regions such as Turkey, Portugal, Spain, Greece, Victoria (Australia), and California (United States) [1]. Wildfires can significantly damage ecological, social, and economic systems. For example, during the substantial drought conditions of 2011 in Texas, fires stemming from 31,457 total sparks burned four million acres and destroyed 2,947 homes [1]. More wildfire catastrophes have occurred since then, notably in California and Australia. The majority of wildfires in the United States are due to human-caused activities. Therefore, it is necessary to identify these human-made threats and develop mitigation strategies accordingly. With increasing residential settlement in wildlands, holistically mitigating these wildfire threats is paramount.

Electric power lines running through these environments pose the risk of igniting potentially catastrophic wildfires [2]. For example, the Pacific Gas and Electric Company (PG&E), California's largest utility, indicated that one of its aging transmission lines was the likely ignition source for the 2018 Camp Fire [3]. The Wall Street Journal reports that PG&E's electric infrastructure has sparked 1,500 fires since 2014 [2].

To reduce the risk of wildfire ignitions, the California Public Utilities Commission approved the Public Safety Power Shutoff (PSPS) program that permits the de-energization of power lines. Under the PSPS program, customers could lose power during times when forecasts predict severe weather with respect to wildfire conditions. Utilities usually make decisions regarding line de-energization by using seven-day weather forecasts and the Fire Potential Index (FPI). FPI is a metric that quantifies whether vegetation in an area is dry enough to burn and sustain a wildfire. FPI is high when moisture in the air is low [4]. In October 2019, the PSPS program disconnected up to three million people from power for as long as 72 hours. Hence, the program was subject to intense backlash and criticism from customers and government officials [2], [3].

Many electricity-related wildfire ignitions are associated with power line faults via vegetation contact. High current flows through power lines exacerbate line sagging and hence reduce clearances between the conductors and nearby vegetation. Thus, high current flows increase the likelihood of vegetation-contact faults that can ignite wildfires. The Nuns Fire in 2017 is an example of a wildfire ignited by vegetation contact [3]. The California Department of Forestry and Fire Protection blamed sagging power lines as the cause of this fire [5].

To manage the risk of faults due to vegetation contact, utility companies specify ground clearance requirements for their transmission lines. These clearance requirements are often based on the lines' nominal voltages [6].

In this paper, we aim to mitigate the risk of wildfire ignition by imposing more stringent ground clearance requirements for transmission lines. We ensure satisfaction of these clearance requirements using a so-called *Dynamic Line Rating* (DLR) approach that adjusts the line flow limits using short-term forecasts or real-time measurements of the ambient conditions for each line. To characterize the potential benefits of this approach, we compare the combination of more stringent ground clearance limits and DLR to an alternative strategy of de-energizing the lines that pose a high risk of igniting wildfires.

Compared to infrastructure hardening strategies, such as undergrounding transmission lines, DLR provides an inexpensive approach for mitigating wildfire-ignition risks. Moreover, as we will show via case studies, the combination of more stringent ground clearance requirements along with DLR can significantly reduce load shedding relative to a line de-energization strategy. Thus, the study conducted in this paper characterizes potential advantages of a DLR strategy. Highlighting our results, a case study combining a large-scale (10,000-bus) dataset

representative of Western Electricity Coordinating Council (WECC) with actual data regarding ambient conditions, load demands, and wildfire risks indicates that the proposed DLR approach can significantly reduce load shedding relative to an alternative approach which de-energizes lines that pose high risks of igniting wildfires.

The significant reduction in load shedding from the proposed DLR approach motivates further analysis to quantify the amount of wildfire risk reduction achieved by various ground clearance requirements. Several relevant steps in this direction are provided in [7], [8], [9]. However, future work is needed to fully characterize the precise implications of various transmission line operational conditions with respect to wildfire-ignition risks.

We also note that the DLR strategy in this paper fits into broader efforts by the power systems research community regarding wildfires. Researchers have proposed methods for determining what equipment is at highest risk, collected historical data regarding wildfires and their grid impacts, modeled the impacts of fires on utility assets, identified wildfire risks to the grid, and determined risk indicator metrics for equipment and nearby resources [10], [11]. Other related work investigates the use of fault-current limiters for wildfire-risk reduction [12]. Additionally, power systems researchers have recently proposed an optimal transmission line switching strategy that selectively de-energizes high-risk transmission lines while minimizing the required load shedding [13]. An important direction for future work involves comparing various approaches for mitigating wildfire ignition risks.

The rest of this paper is organized as follows. Section II provides an overview of DLR applications. Section III presents the mathematical formulation of our DLR approach for determining current flow limits based on conductor features, ambient temperatures, target conductor temperature, and time of day. Section IV formulates an AC optimal power flow (AC OPF) problem and a DC unit commitment (DC UC) problem that use dynamic line ratings to satisfy ground clearance requirements by managing the amount of line sagging. Section V describes and analyzes two illustrative case studies. Finally, Section VI concludes the paper and discusses future work.

II. Overview of Dynamic Line Rating

System operators enforce limits on the amount of current allowed to flow through transmission lines during steady-state conditions. These limits are based on the ampacity of the conductor material, the amount of line sag permissible while satisfying ground clearance requirements, and system-wide requirements determined by contingency analysis, transient stability, and other system security applications. This paper considers line flow limits as determined by ground clearance requirements. Ground clearance requirements may restrict operation below the limits associated with the conductors' material characteristics. As an example, consider lines composed of aluminum-stranded conductor steel-reinforced (ACSR) material whose maximum allowable temperature is 90°C [14]. To satisfy ground clearance requirements, these lines are often operated with current flows that result in conductor temperatures between 40°C and 75°C [14].

System operators commonly use Static Line Ratings (SLR) for transmission line limits. SLR are changed infrequently (e.g., seasonally) according to worst-case assumptions regarding ambient conditions such as temperature and wind speed. Since SLR do not account for real-time ambient conditions, they do not always represent the actual line capacities.

In contrast, DLR techniques account for real-time ambient conditions such as temperature and wind speed in order to more accurately characterize the permissible line flows [15], [16]. Prior applications of DLR have primarily focused on unlocking additional capacity on power lines to mitigate grid congestion. DLR approaches can also be used to avoid expensive installations of new lines or conductor upgrades [15], [16]. We propose the use of DLR for the alternative purpose of managing the risks of wildfire ignition from transmission lines. We specifically compare the de-energization of transmission lines versus the use of DLR to enforce more stringent ground clearance requirements while considering time-varying ambient conditions.

III. Approach for Calculating Dynamic Line Ratings

To mitigate wildfire ignition risk, we propose a DLR approach that quantifies line current limits based on the maximum permitted line sag using conservative ground clearances recommended by the US Forest Service. The permitted sag determines the respective target conductor temperatures using a mathematical formulation applicable to ACSR conductors. Once the maximum conductor temperatures are known, we calculate the lines' flow limits using the IEEE-738 standard [17].

A. Ground Clearance Recommendations

Currently, the California Public Resource Code (CPRC) recommends clearance of all vegetation for a specific radial distance from a conductor. This clearance varies with the conductor's nominal voltage. For example, vegetation clearance requirements are 1.2 m for 2.4 kV to 72 kV lines, 1.8 m for 72 kV to 110 kV lines, and 3 m for all line voltages above 110 kV in high-fire-threat districts [6].

Ground clearance requirements protect public safety and improve electric system reliability. These requirements are intended to prevent fire ignition due to arcing from conductors to ground, to other conductors, and to surrounding vegetation in forest-covered land. Table I shows the clearance distances proposed in a US Forest Service study [6] for various vegetation types (e.g., grass, brush, forest trees) and pole materials (steel, aluminum, fiberglass, and wood). These ground clearances, which are intended to protect electrical equipment during a wildfire event, are more stringent than recommended clearances from CPRC. In our case studies, we impose the more stringent clearance requirements in Table I to increase the distance between electrical equipment and surrounding vegetation.

TABLE I
CLEARANCES RECOMMENDED BY THE US FOREST SERVICE STUDY [7]

Tower material	30 m tall crown fire clearance
Wood	20 m
Steel	5 m
Aluminum	5 m
Fiberglass	15 m

B. Maximum Allowable Line Sag and Conductor Temperature

The maximum allowable line sag is computed by subtracting the ground clearances in Table I [6] from transmission tower heights, which are available via documentation from California utilities [18]. The next step in translating the maximum allowable line sag into a current flow limit requires the relationship between the line sag and the conductor temperature. Studies conducted by CIGRE yield the relationship between conductor temperature and line sag [19]. Fig. 1 shows this relationship for ACSR conductors.

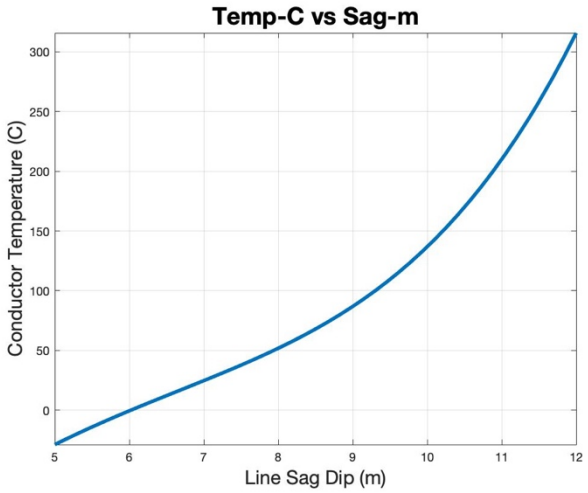

Fig. 1. Relationship between conductor temperature (*y*-axis) and line sag (*x*-axis) [19].

C. Current-Temperature Relationship for a Conductor

The IEEE-738 standard for Calculating the Current-Temperature of Bare Overhead Conductors [17] provides a method to determine the current that produces the maximum allowable conductor temperature as well as the conductor temperature associated with a specified current. The conductor temperature is a function of conductor-specific physical properties such as material and diameter; ambient conditions such as temperature, wind speed, solar insolation; and heating from resistive losses due to the current flow through the conductor.

The DLR computations in this paper are based on the steady-state model in the IEEE-738 conductor temperature standard [17]. Table II gives the nomenclature for the parameters used in the equations that follow.

TABLE II
PARAMETERS FOR DLR CALCULATIONS

Symbol	Description	Units
Conductor		
A'	Area of conductor per length	m^2/m
D	Diameter of conductor	mm
T_c	Conductor Temperature	°C
$R(T_c)$	Resistance of conductor at temperature T_c	Ω/m
Solar properties – dependent on the location and time of day		
Q_s	Total solar and sky radiated heat flux rate	W/m^2
H_C	Altitude of sun	degrees
Z_c	Azimuth of sun	degrees
Z_l	Azimuth of line	degrees
δ	Solar declination	degrees
Weather		
T_A	Ambient temperature	°C
V_w	Wind speed	m/s
Atmosphere		
$k_f(T_A,T_C)$	Thermal conductivity of air based on T_A, T_C	W/(m-°C)
$\mu_f(T_A,T_C)$	Dynamic viscosity at based on T_A, T_C	$P_a \bullet s$
$\rho_f(T_A,T_C)$	Air density based on T_A, T_C	kg/m^3

We consider current flow limits that depend on the maximum allowable conductor temperature. Temperature characteristics for ACSR conductors are available from 50°C to 180°C [20]. To compute the conductor temperature, we use the equation for steady-state heat balance [17]:

$$I^2 R_{T_C} + q_s = q_c + q_r \quad (1)$$

Here, I is the current flowing through the conductor, R_{Tc} is the conductor resistance at T_C, q_s is the solar heat gain, and q_c and q_r are the convection and radiative heat losses, respectively. We compute heat losses and gains using the formulas provided in (2)–(5) as discussed in [17].

- The heat gain from solar irradiance on the conductor surface, q_s, is:

$$q_s = \alpha Q_s A' \sin(\eta), \quad (2)$$

where $\eta = \arccos\left[\cos(H_c)\cos(Z_C - Z_l)\right]$, which depends on the sun's position at any particular time. The exact solar absorptivity is dependent on the conductor age and the pollution level [21]. In our case studies, we select $\alpha = 0.5$.

- At low wind speeds, the cooling effect from the wind is given by the convective heat loss equation:

$$q_c = K_{\varphi_w} k_f (T_C - T_A)\left[1.01 + 0.371\left(\frac{D\rho_f V_w}{\mu_f}\right)^{0.52}\right]. \quad (3)$$

In (3), K_{φ_w} is a function of the angle φ_w between the conductor orientation and the wind direction: $K_{\varphi_w} = 1.194 - \cos(\varphi_w) + 0.194\cos(2\varphi_w) + 0.368\sin(2\varphi_w)$. Without knowledge of the lines' precise geographic orientations, the case studies in this paper consider a perpendicular wind direction to the conductor axis, leading to a value of $K_{\varphi_w} = 1.0$. The case studies also consider low wind speeds in the surrounding environment.

- The release of heat into the conductor's surroundings has a radiative cooling effect, modeled as q_r:

$$q_r = 0.138 D\varepsilon\left[\left(\frac{T_C+273}{100}\right)^4 - \left(\frac{T_A+273}{100}\right)^4\right]. \quad (4)$$

We consider an emissivity value of $\varepsilon = 0.5$ in our case studies. Note that k_f, ρ_f, μ_f are all dependent on T_C and T_A.

D. Determining Line Flow Limits

After calculating the maximum acceptable line sag, we compute the corresponding dynamic line flow limits using (1)–(4). Contrary to SLR approaches which employ worst-case assumptions for the ambient conditions (wind, solar irradiance, temperature) over an extended period, DLR limits are adaptable to time-varying ambient conditions.

The paper uses real data on spatially and temporally varying wildfire risks to identify the lines that are most prone to igniting wildfires. For these high-risk lines, we use DLR to compute line flow limits that result in line sags which satisfy the stricter ground clearance requirements in Table I.

IV. Power System Optimization Problems

In this section, we apply the limits computed by the DLR approach from Section III to both an AC optimal power flow problem and a DC unit commitment problem. For both problems,

the objective function and constraints are formulated in a traditional manner with the exception of current flow limits I_l^{dmax} that are computed dynamically based on the ambient conditions as described in Section III.

A. AC Optimal Power Flow with Dynamic Line Ratings

Let *G, N,* and *L* denote the sets of generators, buses, and lines, respectively. For each generator $i \in G$, consider a convex quadratic generation cost function with coefficients c_{2i}, c_{1i}, and c_{0i}. Load shedding is permitted at a high cost denoted by β. The AC OPF problem is:

$$\min \sum_{i\in G}(c_{2i}P_{G_i}^2 + c_{1i}P_{G_i} + c_{0_i}) + \beta \sum_{i\in N} P_{shed,i} \qquad (5)$$

subject to:

(for all $i \in N$)

$$P_{Gi} - P_{Di} + P_{shed,i} - V_i^2 g_{sh,i} = \sum_{l\in A_i} P_l(V,\theta) \quad \text{Bus Active Power Balance}$$

$$Q_{Gi} - Q_{Di} + \alpha_i P_{shed,i} + V_i^2 b_{sh,i} = \sum_{l\in A_i} Q_l(V,\theta) \quad \text{Bus Reactive Power Balance}$$

$$0 \le P_{shed,i} \le P_{Di} \quad \text{Allowable Load Shed Range}$$

$$V_i^{min} \le V_i \le V_i^{max} \quad \text{Voltage Magnitude Limits}$$

(for all $l \in L$)

$$|I_l(V,\theta)| \le I_l^{dmax} \quad \text{Dynamic Line Limits}$$

(for all $i \in G$)

$$P_{Gi}^{min} \le P_{Gi} \le P_{Gi}^{max} \quad \text{Active Power Limits}$$

$$Q_{Gi}^{min} \le Q_{Gi} \le Q_{Gi}^{max} \quad \text{Reactive Power Limits}$$

$$\theta_1 = 0^\circ \quad \text{Angle Reference}$$

where $P_l(V,\theta)$, $Q_l(V,\theta)$ and $|I_l(V,\theta)|$ denote the active power flow, the reactive power flow, and the magnitude of the current flow on line *l,* respectively, as functions of the voltage magnitudes and angles, V and θ (i.e., the power flow equations for line *l*); the set A_i contains the lines connected to bus *i*; P_{G_i} and Q_{G_i} are the active and reactive power outputs for generator *i*; P_{D_i} and Q_{D_i} are the active and reactive power demands at bus *i*; $g_{sh,i}$ and $b_{sh,i}$ are the shunt conductance and susceptance at bus *i;* the variable $P_{shed,i}$ corresponds to the amount of load shed at bus *i*; α_i is a constant corresponding to a fixed power factor for the load shed at bus *i;* and superscripts *max* and *min* indicate upper and lower bounds on the corresponding quantities.

We implement our case study simulations using the power system software package MATPOWER version 7.1 [22].

B. DC Unit Commitment with Dynamic Line Ratings

We also consider the application of DLR to DC unit commitment problems in order to mitigate the risk of wildfire ignition. Let *T* denote the number of time periods. We minimize the sum of the fixed costs (c_{0it}), convex quadratic production costs (c_{2it} and c_{1it}), startup costs (c_{it}^{SU}), and shutdown costs (c_{it}^{SD}) totaled over each generator i and time period t. This formulation also permits load shedding at a high cost (β), with the variable $P_{shed,it}$ denoting the load shed at bus *i* in period *t*. Similar to the AC OPF problem in (5), the key distinctions with respect to a traditional DC UC formulation are dynamically computed current flow limits I_l^{dmax} that are based on the ambient conditions as described in Section III. The resulting unit commitment problem is:

$$\min \sum_{t=1,\dots,T}\sum_{i\in G}(c_{2it}P_{Gi}^2 + c_{1it}P_{Gi} + c_{0it}u_{it} + c_{it}^{SU}v_{it} + c_{it}^{SD}w_{it}) + \sum_{t=1,\dots,T}\sum_{i\in N}\beta P_{shed,it} \qquad (6)$$

subject to:

(for all $i \in N$ and $t = 1, \dots, T$)

$$P_{Git} - P_{Dit} + P_{shed,it} = \sum_{l\in A_i} P_l(\theta_t) \quad \text{Bus Power Balance}$$

$$0 \le P_{shed,it} \le P_{Dit} \quad \text{Allowable Load Shed Range}$$

(for all $l \in L$ and $t = 1, \dots, T$)

$$-I_l^{dmax} \le P_l(\theta_t) \le I_l^{dmax} \quad \text{Dynamic Line Limits}$$

(for all $i \in G$ and $t = 1, \dots, T$)

$$P_{Gi}^{min}u_{it} \le P_{Git} \le P_{Gi}^{max}u_{it} \quad \text{Power Generation Limits}$$

(for all $i \in G$ and $t = 2, \dots, T$)

$$P_{Git} - P_{Gi,t-1} \le P_i^{RU} \quad \text{Ramp Up Limits}$$

$$P_{Git} - P_{Gi,t-1} \ge -P_i^{RD} \quad \text{Ramp Down Limits}$$

$$u_{it} - u_{i,t-1} = v_{it} - w_{it} \quad \text{Startup and Shutdown Events}$$

$$\theta_1 = 0^\circ \quad \text{Angle Reference}$$

For time period *t*, P_{Dit} denotes the active power demand at bus *i*; P_{Git} is the active power output for generator *i;* P_i^{RU} and P_i^{RD} are specified bounds on the ramp up and ramp down rates for generator *i*; and $P_l(\theta_t) = \frac{1}{X_l}(\theta_{l_o t} - \theta_{l_d t})$ is the DC approximation for active power flow through the line *l* with origin bus l_o, destination bus l_d, and series reactance X_l, where θ_{it} is the voltage angle for bus *i*. The binary variable u_{it} indicates the on/off status of generator *i* at time *t*. The binary variables v_{it} and w_{it} indicate whether generator *i* turns on or off, respectively, at time period *t*. Note that we formulate the current flow limits by bounding the power flow variables $P_l(\theta_t)$ that are available in the DC approximation by I_l^{dmax}, converted to per unit representation.

We implement our DC unit commitment case study simulations using the power system software package MATPOWER MOST version 1.1 [23] and use Gurobi's mixed-integer quadratic programming solver to compute the optimal operating points.

V. CASE STUDIES

This section demonstrates the potential advantages of using DLR to mitigate wildfire ignition risks via two case studies.

A. Case Study 1: AC OPF for the IEEE 14-Bus System

1) *Ground Clearance and Ambient Conditions.* Based on Table I, we select a minimum ground clearance of 35 m. The average height of lattice steel towers is 43 m [24]. Hence, we enforce a maximum allowable sag of 7 m for this case study.

For the ambient conditions, we consider a wind speed (V_w) of 5 miles per hour (2.235 m/s) and a temperature (T_a) of 40°C.

2) Power System Dataset. We analyze the power flows for the PGLib-OPF version of the IEEE 14-bus system [25] that is shown in Fig. 2. We consider the case where the three lines marked with yellow symbols pose high risks for igniting wildfires. The entire system operates at 69 kV. We consider lines with ACSR 26/7 conductors that have diameter (D) of 28.1 mm and resistances (R_{20C}) of 0.0214 Ω/kft. We consider a location for this test case in California with the following geographical parameters: latitude of 39.7°N, longitude of 121.8°W; and solar altitude (H_C) 47.6°. We use this information to calculate the position of the sun as used in (2) [17].

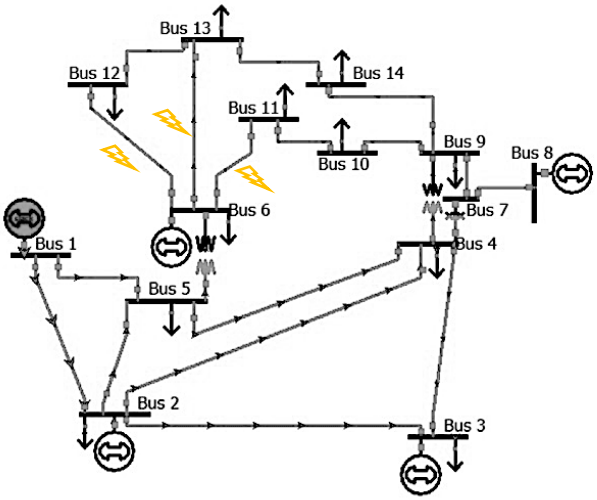

Fig. 2. One-line diagram for the IEEE 14-bus test case from [25]. The yellow symbols represent lines at high risk of igniting wildfires.

3) Comparisons. We compare two options for reducing the risk of wildfire ignition. The first option de-energizes the three high-risk lines to emulate the PSPS program. All other lines have flow limits that ensure line sags do not violate the ground clearance requirements from CPRC [19]. We assume that the other lines pose no risk of sparking a wildfire. We compare this de-energization option to an alternative DLR option where a conservative 8 m clearance requirement is enforced instead of de-energizing these lines. We calculate line current limits using (1)–(4) and the specified ambient conditions. For both options, we solve the AC OPF problem (5) to compute the least-cost operating points that satisfy all constraints.

4) *Results.* De-energizing the high-risk lines leads to shedding 5% of the total load. In contrast, enforcing conservative ratings computed using DLR for the high-risk lines enables the total demand to be satisfied (no load shedding). Moreover, Fig. 3 illustrates that the least-expensive generator (generator 1) is capable of serving all of the load when using the DLR limits, whereas de-energization of the high-risk lines leads to the dispatch of more expensive power from generator 2.

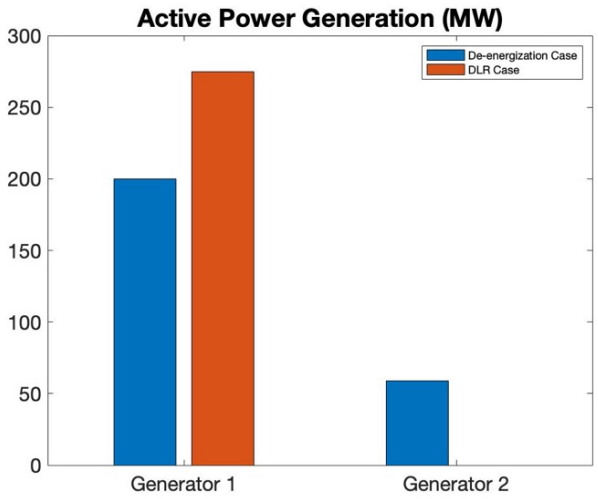

Fig. 3. Comparison of active power generation for the de-energization case and DLR case.

B. Case Study 2: DC Unit Commitment for a 10,000-bus test system representing WECC

1) Ground Clearance and Ambient Conditions. As in the first case study, we select a minimum ground clearance of 35 m based on Table I. We again consider an average height of lattice steel towers of 43 m [24] and thus also enforce a maximum allowable sag of 7 m for the high-risk lines in this case study.

For the ambient conditions, we exploit the geographic data provided in the second test case to compute actual ambient conditions. Specifically, we use wind speed (V_w), solar radiation (Q_s) and temperature (T_a) values available from the California Irrigation Management Information System (CIMIS). CIMIS has 145 weather stations installed across California that measure the aforementioned weather data on a minute-by-minute basis, thus enabling the use of actual ambient conditions for the case study [26]. The locations for each line are estimated using the midpoint of the line's terminal locations. We select September 1, 2020 as the date for our case study, using the corresponding actual ambient conditions observed on this date. September 1 is during the most dangerous period of the wildfire season in California and has historically had PSPS events, thus making this date an appropriate subject of our analysis.

2) Power System Dataset. Our second case study analyzes the effects of applying DLR techniques to a 10,000-bus synthetic test case that is representative of the WECC system in the Western United States [27], [28]. The test case's load variation is temporally scaled according to the actual California load profile data shown in Fig. 5 [29].

Using knowledge of the geographic locations in this dataset, we compute current flow limits using the DLR approach described in Section III for all lines that are considered risky enough to ignite a wildfire. When computing these limits, we use actual geographically and temporarily varying data regarding ambient conditions on the date selected for this case study (September 1, 2020). Fig. 4 shows a representative example of the time variation for one such flow limit. Note that the flow limits are selected as the minimum of the DLR value and the

conductor's ampacity limit associated with the material properties, leading to the cutoff at 907 A in the figure.

We also use actual Fire Potential Index data from the study date [4]. Fig. 6 shows the distribution of normalized FPI values associated with each line in the 10,000-bus system. We selected the 35 lines with the largest FPI values as the high-risk lines for our analysis.

3) *Comparisons.* We compare the same two approaches for reducing the risk of wildfire ignition: de-energizing the high-risk lines (during all time periods) versus using the proposed DLR approach to compute line flow limits corresponding to conservative ground clearances for these lines. (Flow limits for the remaining lines are adopted from the original dataset.) For both approaches, we solve the DC UC problem (6) with 24 hourly time intervals to compute the least-cost operating points that satisfy all constraints.

4) Results. The case study results are shown in Fig. 7. The vertical axis in this figure indicates the amount of load shedding resulting from the de-energization approach as a fraction of the total load. The horizontal axis corresponds to the time periods (24 hours). Note that the DLR approach does not require more than 0.01% load shedding in any time period. Compared to the nearly 50% load shedding required during certain time periods for the de-energization approach, the DLR approach reduced load shedding by nearly 50% of the peak demand in this case.

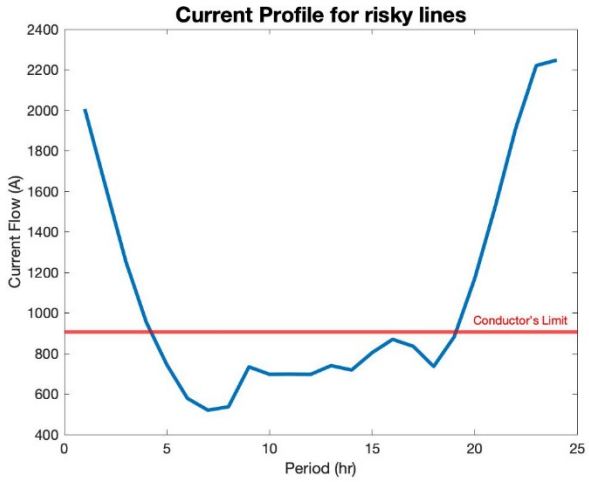

Fig. 4. A representative example of a temporally varying flow limit from the DLR approach.

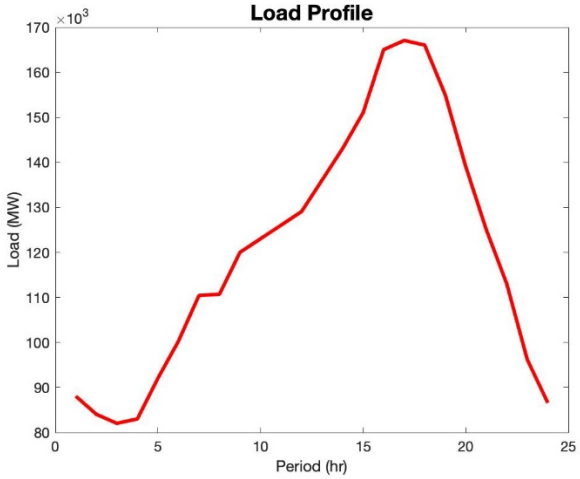

Fig. 5. Load demand profile for California [29].

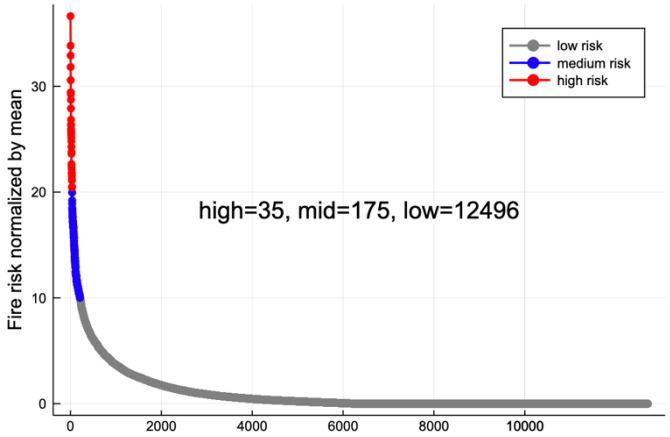

Fig. 6. Illustration of the lines at risk of igniting wildfire for 10,000-bus system according to their associated FPI values [4].

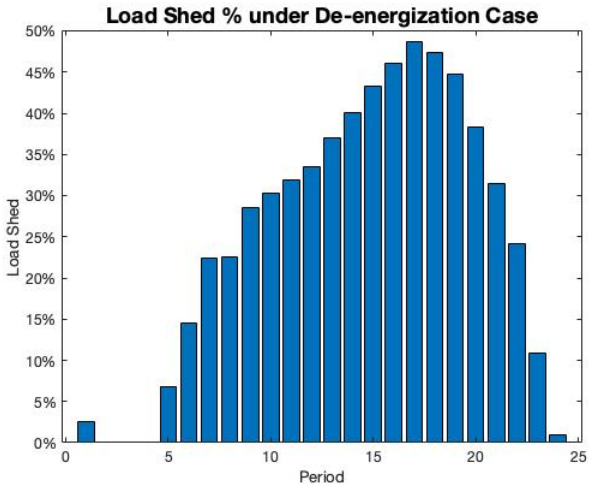

Fig. 7. Load shed as a percentage of the total load for the de-energization option in the 10,000-bus system as a function of time (hours). The load shed from the DLR approach is less than 0.01% for all time periods.

C. Case Study Summaries

Both case studies indicate that enforcing strict ground clearance requirements using a DLR approach can substantially reduce load shedding relative to de-energizing transmission lines that pose high risks of igniting wildfires. The results of our second case study, in particular, highlight this finding, as the DLR approach nearly eliminates the significant amount of load shedding from line de-energization. By considering actual recorded data, we emphasize that this case study captures the related impacts of ambient conditions on load demands, wildfire-ignition risks, and DLR limits. The promising results of this realistic case study motivate further investigation regarding the potential application of DLR for mitigating the risk of igniting wildfires.

VI. Conclusions

Limiting line sag by following conservative ground clearances in certain areas leads to lower power flows on lines that are at risk of igniting wildfires. Using a DLR approach, we enforce these flow limits in AC optimal power flow and DC unit commitment problems. Two case studies demonstrate that enforcing DLR limits on high fire-threat lines rather than de-energizing them can significantly reduce load shedding. These

results motivate further investigation regarding the degree to which imposing more conservative ground clearance requirements reduce the risks of wildfire ignition.

Other future work includes additional analyses regarding the practical applicability of DLR approaches for mitigating wildfire-ignition risks, such as extension to security-constrained unit commitment problems. Similar analyses with stochastic unit commitment problems would enable consideration of the correlated impacts of uncertainties in ambient conditions with respect to load demands, renewable generation, and DLR limits.

ACKNOWLEDGEMENT

The authors gratefully acknowledge the assistance of Alyssa Kody in obtaining and interpreting the Fire Protection Index data used in Section V-B.

VII. REFERENCES

[1] M.J. Erickson, J.J. Charney and B.A. Colle, "Development of a Fire Weather Index using Meteorological Observations within the Northeast United States", *Journal of Applied Meteorology and Climatology*, vol. 55, no. 2, pp. 389-402, 2016.

[2] R. Gold, K. Blunt, and R. Smith, "PG&E Sparked at Least 1,500 California Fires. Now the Utility Faces Collapse," *The Wall Street Journal*, 13-Jan-2019. [Online]. Available: https://www.wsj.com/articles/pg-e-sparked-at-least-1-500-california-fires-now-the-utility-faces-collapse-11547410768. [Accessed: 15-Dec-2020].

[3] R. Gold, R. Rigdon, Y. Serkez, and D. Cole, "How PG&E's Aging Equipment Puts California at Risk," *The Wall Street Journal*, 29-Oct-2019. [Online]. Available: https://www.wsj.com./graphics/california-wildfire-pge-drought/. [Accessed: 26-Feb-2021].

[4] M. Jolly, "Large Fire Potential and Fire Potential Indexes," The Wildland Fire Assessment System (WFAS). [Online]. Available: https://www.wfas.net/index.php/large-fire-potential-and-fire-potential-indexes-external-products-107. [Accessed: 15-Dec-2020].

[5] D. Kasler, "PG&E Gets Blamed for Another Deadly 2017 Wildfire, this Time from 'Sagging Power Lines*,'" The Sacramento Bee, 2018*. [Online]. Available: https://www.sacbee.com/news/california/fires/article219731815.html. [Accessed: 28-Jan-2021].

[6] B.W. Butler, J. Webb, J. Hogge, and T. Wallace, "Vegetation Clearance Distances to Prevent Wildland Fire Caused Damage to Telecommunication and Power Transmission Infrastructure," *Large Wildland Fires Conference*, Missoula, MT, May 2014.

[7] J. W. Mitchell, "Power Line Failures and Catastrophic Wildfires under Extreme Weather Conditions," *Engineering Failure Analysis,* vol. 35, pp.726–735, 2013.

[8] J. E. Keeley and A. D. Syphard, "Historical Patterns of Wildfire Ignition Sources in California Ecosystems," *International Journal of Wildland Fire*, vol. 27, no. 12, pp. 781–799, 2018.

[9] M. Williamson, "Application of Distributed Solar Photovoltaics and Energy Storage to Mitigate Bushfire Risk in Victoria, Australia," Masters Thesis, Centre for Renewable Energy Systems Technology (CREST), Loughborough University, 2015.

[10] L. Dale, M. Carnall, M. Wei, G. Fitts, and S. McDonald, "Assessing the Impact of Wildfires on the California Electricity Grid," *California's Fourth Climate Change Assessment*, Energy Commission Study CCCA4-CEC-2018-002, Aug. 2018.

[11] J.H. Scott, M.P. Thompson, and D.E. Calkin, "A Wildfire Risk Assessment Framework for Land and Resource Management," Tech. Rep. RMRS-GTR-315, U.S. Department of Agriculture, Forest Service, Rocky Mountain Research Station, Oct. 2013.

[12] T.K. Roy, M.A. Mahmud, S.K. Ghosh, M.A.H. Pramanik, R. Kumar, and A. M. T. Oo, "Design of an Adaptive Sliding Mode Controller for Rapid Earth Fault Current Limiters in Resonant Grounded Distribution Networks to Mitigate Powerline Bushfires," *Texas Power and Energy Conference (TPEC)*, February 2021.

[13] N. Rhodes, L. Ntaimo and L.A. Roald, "Balancing Wildfire Risk and Power Outages through Optimized Power Shut-Offs," to appear in *IEEE Transactions on Power Systems,* 2021.

[14] S.D. Kim and M.M. Morcos, "An Application of Dynamic Thermal Line Rating Control System to Up-Rate the Ampacity of Overhead Transmission Lines," *IEEE Transactions on Power Delivery*, vol. 28, no. 2, pp. 1231-1232, April 2013.

[15] J. Teh, C. Lai, N.A. Muhamad, C.A. Ooi, Y. Cheng, M.A.A. Mohd Zainuri, and M.K. Ishak, "Prospects of Using the Dynamic Thermal Rating System for Reliable Electrical Networks: A Review," *IEEE Access*, vol. 6, pp. 26765-26778, 2018.

[16] D. L. Alvarez, J. A. Rosero, F. Faria da Silva, C. L. Bak and E. E. Mombello, "Dynamic Line Rating — Technologies and Challenges of PMU on Overhead Lines: A Survey," *51st International Universities Power Engineering Conference (UPEC)*, Coimbra, 2016, pp. 1-6.

[17] "IEEE Standard for Calculating the Current-Temperature Relationship of Bare Overhead Conductors," in IEEE Std 738-2012 (Revision of IEEE Std 738-2006 - Incorporates IEEE Std 738-2012 Cor 1-2013), pp.1-72, December 23, 2013.

[18] "Manage Trees and Plants Near Power Lines," Laws and regulations. [Online]. Available: https://www.pge.com/en_US/safety/yard-safety/powerlines-and-trees/laws-and-regulations.page. [Accessed: 28-Dec-2020].

[19] R. Stephen, T. Seppa, D. Douglass, M. Lancaster, G. Biedenbach, G. Watt, J.L. Lilien, R. Pestana, P. Ferrieres, and M. Schmale, "CIGRE Guide for Application of Direct Real-Time Monitoring Systems," Cigré, 2012.

[20] T. Barton and P. Musilek, "Day-Ahead Dynamic Thermal Line Rating Using Numerical Weather Prediction," *IEEE Canadian Conference of Electrical and Computer Engineering (CCECE)*, Edmonton, AB, Canada, 2019.

[21] M. Bockarjova and G. Andersson, "Transmission Line Conductor Temperature Impact on State Estimation Accuracy," *IEEE Lausanne PowerTech*, Lausanne, Switzerland, pp. 701-706, 2007.

[22] R.D. Zimmerman, C.E. Murillo-Sanchez, and R.J. Thomas, "MATPOWER: Steady-State Operations, Planning and Analysis Tools for Power Systems Research and Education," *IEEE Transactions on Power Systems*, vol. 26, no. 1, pp. 12–19, Feb. 2011.

[23] C.E. Murillo-Sanchez, R.D. Zimmerman, C.L. Anderson, and R.J. Thomas, "Secure Planning and Operations of Systems with Stochastic Sources, Energy Storage and Active Demand," *IEEE Transactions on Smart Grid*, vol. 4, no. 4, pp. 2220–2229, Dec. 2013.

[24] R. Benato, R. Caldon, M. Coppo, S. Dambone Sessa, D. Mimo, D. Peroni, and M. Previatello, "Highly Efficient Overhead Line Innovative Conductors with Reduced Joule Power Losses," *AEIT International Annual Conference*, Cagliari, 2017, pp. 1-6.

[25] S. Babaeinejadsarookolaee, A. Birchfield, R.D. Christie, C. Coffrin, C.L. DeMarco, R. Diao, M. Ferris, S. Fliscounakis, S. Greene, R. Huang, C. Josz, R. Korab, B.C. Lesieutre, J. Maeght, D.K. Molzahn, T.J. Overbye, P. Panciatici, B. Park, J. Snodgrass, and R.D. Zimmerman, "The Power Grid Library for Benchmarking AC Optimal Power Flow Algorithms," IEEE PES PGLib-OPF Task Force Report, *arXiv:1908.02788*, Aug. 2019.

[26] "CIMIS Weather Station Data," *California Natural Resources Agency Open Data*. [Online]. Available: https://data.cnra.ca.gov/dataset/cimis-weather-station-data. [Accessed: 02-Feb-2021].

[27] T. Xu, A. B. Birchfield, and K. S. Shetye; T. J. Overbye, "Creation of Synthetic Electric Grid Models for Transient Stability Studies," *IREP Symposium Bulk Power System Dynamics and Control X*, Espinho, Portugal, August 2017.

[28] T. Xu, A. B. Birchfield and T. J. Overbye, "Modeling, Tuning and Validating System Dynamics in Synthetic Electric Grids," *IEEE Transactions on Power Systems*, vol. 33, no. 6, pp. 6501-6509, November 2018.

[29] "CAISO: Actual Load - LCG Consulting," EnergyOnline. [Online]. Available: http://www.energyonline.com/Data/GenericData.aspx?DataId=18. [Accessed: 05-Mar-2021].